HHS Public Access

Author manuscript

Circ Res. Author manuscript; available in PMC 2022 January 15.

Published in final edited form as:

Circ Res. 2014 August 01; 115(4): 450–459. doi:10.1161/CIRCRESAHA.115.304262.

OxLDL Triggers Retrograde Translocation of Arginase 2 in Aortic Endothelial Cells via ROCK and Mitochondrial Processing Peptidase

Deepesh Pandey[1], **Anil Bhunia**[1], **Young Jun Oh**[1], **Fumin Chang**[1], **Yehudit Bergman**[1], **Jae Hyung Kim**[1], **Janna Serbo**[1,2], **Tatiana N. Boronina**[6], **Robert N. Cole**[6], **Jennifer Van Eyk**[7], **Alan T. Remaley**[8], **Dan E. Berkowitz**[#1,2], **Lewis Romer**[#1,2,3,4,5]

[1]Anesthesiology and Critical Care Medicine, Johns Hopkins University School of Medicine, Baltimore, MD 21287-4904

[2]Biomedical Engineering, Johns Hopkins University School of Medicine, Baltimore, MD 21287-4904

[3]Cell Biology, Johns Hopkins University School of Medicine, Baltimore, MD 21287-4904

[4]Pediatrics, Johns Hopkins University School of Medicine, Baltimore, MD 21287-4904

[5]Center for Cell Dynamics, Johns Hopkins University School of Medicine, Baltimore, MD 21287-4904

[6]Mass Spectrometry and Proteomics Facility, Johns Hopkins University School of Medicine, Baltimore, MD 21287-4904

[7]Departments of Medicine and Biological Chemistry, Johns Hopkins University School of Medicine, Baltimore, MD 21287-4904

[8]Cardiovascular-Pulmonary Branch, National Heart, Lung, and Blood Institute, National Institutes of Health, Bethesda, MD

[#] These authors contributed equally to this work.

Abstract

Rationale—Increased arginase activity contributes to endothelial dysfunction by competition for L-arginine substrate and reciprocal regulation of NOS. The rapid increase in arginase activity in human aortic endothelial cells (HAEC) exposed to oxidized LDL is consistent with post-translational modification or subcellular trafficking.

Objective—To test the hypotheses that OxLDL triggers reverse translocation of mitochondrial Arginase 2 (Arg2) to cytosol and Arg2 activation, and that this process is dependent upon mitochondrial processing peptidase (MPP), LOX-1 receptor and ROCK.

Address correspondence to: Dr. Lew Romer Johns Hopkins University School of Medicine Charlotte R. Bloomberg Children's Center Suite 6318-C / Pediatric ACCM 1800 Orleans Street Baltimore, MD 21287-4904 Tel: 410-955-7610 Fax: 410-502-5312 LRomer@jhmi.edu.

DISCLOSURES

Dan E. Berkowitz is a scientific founder and consultant for Corridor Pharmaceuticals, Inc., a biotechnology company dedicated to the development of therapeutics targeting arginase in diseases in which endothelial dysfunction is an important contributing factor.

Methods and Results—OxLDL triggered translocation of Arg2 from mitochondria to cytosol in HAEC and in murine aortic intima with a concomitant rise in arginase activity. All of these changes were abolished by inhibition of MPP or by its siRNA-mediated knockdown. ROCK inhibition and the absence of the LOX-1 receptor in KO mice also ablated translocation. Amino-terminal sequencing of Arg2 revealed 2 candidate mitochondrial targeting sequences, and deletion of either of these confined Arg2 to the cytoplasm. Inhibitors of MPP or LOX-1 receptor KO attenuated OxLDL-mediated decrements in endothelial-specific NO production and increases in superoxide generation. Finally, *Arg2*$^{-/-}$ mice bred on an *ApoE*$^{-/-}$ background showed reduced plaque load, reduced ROS production, enhanced NO, and improved endothelial function as compared with *ApoE*$^{-/-}$ controls.

Conclusion—These data demonstrate dual distribution of Arg2, a protein with an unambiguous MTS, in mammalian cells, and its reverse translocation to cytoplasm by alterations in the extracellular milieu. This novel molecular mechanism drives OxLDL-mediated arginase activation, eNOS uncoupling, endothelial dysfunction, and atherogenesis.

Keywords

Atherogenesis; endothelial dysfuction; endothelial nitric oxide synthase; oxidized low-density lipoprotein; mitochondria; arginase; mitochondrial process

INTRODUCTION

Accumulating evidence suggests that oxidized low density lipoprotein (OxLDL) plays an important role in the pathogenesis of atherosclerosis, and this is supported by its abundance in atherosclerotic lesions [1, 2]. A major target for OxLDL-mediated vascular injury in atherogenesis is the aortic intima [3,4]. Most of these effects occur through OxLDL interaction with its lectin-like oxidized low density lipoprotein receptor-1 (LOX-1) [5]. Endothelium plays a major role in the regulation of vascular homeostasis by modulating vasomotor tone, and vascular smooth muscle cell growth and migration. Impaired endothelial function is considered to be an early and critical event in atherosclerosis, causing abnormalities in the arterial wall and plaque formation [6].

An emerging paradigm in NO biology is the concept that Arg reciprocally regulates NOS activity by competing for L-arginine substrate, and effectively inhibiting NO-dependent processes by depleting the substrate pool available for NO biosynthesis [7]. Furthermore, since L-arginine is spatially confined to a minimum of 3 distinct subcellular pools that are regulated by different transporters and enzymes, local concentrations of L-arginine may limit the activity of the different NOS isoforms that are also spatially segregated within the cell [8]. Arg1 and Arg2 are distinct isoforms encoded by different genes [9, 10]. Arg1 has been referred to as the hepatic isoform and catalyzes the final step of the urea cycle, although its expression can be induced in a wide variety of cells and tissues by hypoxia and LPS [11]. Arg2 is the principal form in EC, and has been referred to as the extrahepatic isoform. It provides ornithine for polyamine synthesis, thereby controlling cell proliferation and differentiation [12, 13]. Arg2 also exhibits broad tissue distribution, and is inducible by a variety of factors including LPS, TNFα, and hypoxia [14-17]. The role of Arg2 in endothelial dysfunction has recently been extended to other disorders in animal models

including aging [7], ischemia-reperfusion [18, 19], hypertension [20, 21], balloon vascular injury [22], ischemia reperfusion injury, and atherosclerosis [23]. Our laboratories have demonstrated that OxLDL increases Arg2 activity in HAEC in a rapid, dose-dependent manner that leads to impaired endothelial NO synthesis [24]. However, the signaling pathways that connect Ox-LDL exposure to Arg2 in EC remain incompletely defined. Thrombin increases Arg2 activity in EC via the Rho/ROCK signaling pathway [25], and RhoA may also be important in Ox-LDL-mediated Arg2 activation in EC [26]. Another clue regarding its regulation is that Arg2 contains a putative mitochondrial targeting sequence in its amino terminus. Arg2 is thought to be largely, but not exclusively, confined to mitochondria in quiescent vascular EC, and we have shown that it constrains endothelial NOS activity [27,28]. However, the mechanism by which mitochondrial Arg2 constrains the activity of (predominantly) cytosolic eNOS is unclear. In the current study, we demonstrate that Arg 2 release from mitochondria to cytoplasm triggers NO-dysregulated vascular dysfunction in rapid response to OxLDL exposure.

METHODS

Detailed methods may be found in the online supplement, which includes following:

Arginase activity assay was determined in lysates of HAEC and murine aortic tissue by measuring urea production.

For plaque quantification, vessels were stained with Sudan IV. Aortic roots were then paraffin-embedded, and cross sections were stained with hematoxylin-eosin to evaluate the atherosclerotic lesion area. Image analysis was done with Image J, version 1.42n. Some aortic segments were permeabilized with 0.5% Triton X-100 in 3% paraformaldehyde and then cut open to expose the intima and Arg2 was imaged using a Zeiss 710-NLO confocal unit and Zeiss Zen software.

Ad-shNontargeted, Ad-MPPα, Ad-MPPβ, Ad-shArg1 and Ad-shArg2 encoded viruses were generated using a pAdBLOCK-iT kit (Life Sciences). An adenoviral construct containing GFP Arg2 was constructed by subsequent subcloning of C-terminally GFP epitope-tagged Arg2 into PENTR1a and then into the PDEST destination vector.

For proteomics studies, cytosol and mitochondria were fractionated and immunoprecipitated from EC using Arg2 polyclonal antibody. Gel bands corresponding to both control and Ox-LDL treated samples were excised, digested with Lys-C and subjected to mass spectrometry analysis. Protein identification by liquid chromatography tandem mass spectrometry (LCMS/MS) analysis of peptides was performed using an LTQ ion trap MS (Thermo Fisher Scientific) interfaced with a 2D nanoLC system (Eksigent, Dublin, CA).

Superoxide and NO measurements were determined using the Luminol analog L-012, and a Siever's NO analyzer, respectively.

MPP activity was determined by measuring PINK1 cleavage.

RESULTS

OxLDL activates endothelial Arg2 by triggering its translocation from the mitochondria to the cytosol

Previously, we have shown that exposure of HAEC to OxLDL rapidly increases Arg2 activity [24, 26]. This time course is consistent with translocation between subcellular compartments and/or post-translational modification(s). Serum-starved HAEC were incubated with 50 μg/mL OxLDL for 2 hours. Ox-LDL exposure promoted robust translocation of Arg 2 from mitochondria to the cytosol (Figure 1A). To further confirm that Arg2 is predominantly targeted to mitochondria, FLAG-tagged Arg2 was expressed in HAEC cells (Figure 1C, 1D). Immunofluorescence studies in unstimulated HAEC cells transfected with FLAG-tagged Arg2 also demonstrated that the majority of Arg2 is located in mitochondria (Figure 1E). Arginase activity was also measured in both mitochondrial and cytoplasmic fractions (Figure 1B). Interestingly, arginase activity was substantially increased in the cytosolic fraction of OxLDL-treated HAEC as compared with the activity of mitochondrial Arg2 in untreated cells.

Although we and others have identified Arg2 as the predominant arginase isoform in HAEC, some reports indicate that Arg1 is expressed in endothelial cells [29]. To determine the contribution of individual Arginase isoforms to total arginase activity in HAEC, we individually silenced Arg1 and Arg2 using adenovirally mediated shRNA transduction. Arg2 silencing inhibited total arginase activity to less than 25% of control levels, whereas Arg1 knockdown had very little effect on total HAEC arginase activity (Supplemental Figure IA). Furthermore, we did not detect any Arg1 expression in quiescent HAEC. These findings suggest that the OxLDL-induced increased in total arginase activity in HAEC is almost entirely mediated by Arg2.

To examine OxLDL-triggered translocation of Arg2 from mitochondria to cytosol in real time, we constructed an Arg 2 with a C-terminus epitope GFP tag, and employed live cell imaging with and without OxLDL (Supplemental Figure II and Supplemental Movies I-III). These data corroborated the biochemical findings and demonstrated the dynamics of OxLDL-induced Arg2 cytosolic translocation.

Changes in mitochondrial membrane potential have been shown to be strongly linked to the decompartmentalization of mitochondrial proteins [30], however no change in mitochondrial membrane potential was observed in intact HAEC in response to OxLDL using the fluorescent probe TMRM (Supplemental Figure III).

OxLDL-mediated cytosolic release and activation of endothelial Arg2 are dependent upon the LOX-1 receptor and Rho Kinase activity

We have previously demonstrated that OxLDL-mediated increases in EC Arg activity are dependent on the LOX-1 receptor [26]. Here we measured Arg2 quantity and activity in cytosolic and mitochondrial fractions of primary cultures of aortic endothelial cells isolated from wild type and LOX-1 receptor knock out mice (LOX-$1^{-/-}$) in response to OxLDL. OxLDL failed to induce cytosolic release and activation of Arg2 in aortic EC from

LOX-1$^{-/-}$ mice (Figure 2A and B). This supports our previous finding that LOX-1 mediates acute OxLDL-induced increases in the activity of Arg2 [26].

Our previous data [26] have demonstrated that RhoA and ROCK activation are downstream events in OxLDL-dependent augmentation of Arg2 activity in EC. To define the role of Rho signaling in OxLDL-dependent decompartmentalization and activation of Arg2, we pre-incubated HAEC with the specific Rho kinase (ROCK) inhibitor Y-27632 (10μM Y-27632, 2 hours) which obviated both Ox-LDL-induced cytosolic translocation of Arg2 and the associated increase in arginase activity (Figure 2C and D).

Truncated Arg2 (without the MTS) localizes to the cytoplasm of HAEC

Most nuclear-encoded proteins that are destined to be incorporated into mitochondria possess mitochondrial targeting sequences (MTS). Although it has been shown that Arg2 resides predominantly in mitochondria [27], the MTS for Arg2 is still undefined and bioinformatics-based predictions of MTS of dual targeted genes have shown to be inaccurate [31]. Identification and characterization of the Arg2 MTS was undertaken in order to understand the dual targeting of this protein, and its regulation by the OxLDL stimulus. We employed mass spectrometry and N-terminal sequencing using Edman's degradation analysis. MS analysis indicated that an immunoprecipitated (IP) cytosolic Arg2 from OxLDL-treated HAEC is cleaved at the His amino acid residue at position 24 (Figure 3A). MS analysis of an IP of Arg2 from the cytosolic fraction of HAEC that were treated with OxLDL provided 30% amino acid sequence coverage at 95% confidence, and yielded the fragmentation spectrum shown in Figure 3A. Since the N-terminus of this Arg2 peptide is not a LysC cleavage site, the N-terminal position of this sequence indicates that the Arg2 parent protein was cleaved (by an endogenous peptidase), leaving HSVAVIGAPFSQGQK as the N-terminal peptide, rather than the traditional LysC site (SVHSVAVIGAPGSQGQK). To further investigate the amino acid(s) that form the N-terminus of full-length Arg2, Edman degradation analysis was carried out on immuno-enriched C-terminal Flag-Arg2 isolated from 293 cells. The N-terminal amino acid sequences obtained were from two peptides, VHSVAVIG, and GQKRKGVEH. These data indicate potential cleavage sites between amino acids 22 and 23 and 35 and 36, respectively (Figure 3B). The second of these potential cleavage sites detected with Edman degradation was consistent with canonical sequences associated with cleavage by the mitochondrial processing peptidase (MPP), as it included arginine residues at positions -2 and -3 relative to the candidate site of cleavage [32]. To evaluate whether deletion of these putative MTS had functional consequences for Arg 2 localization, we generated two N-terminal truncation mutants of Arg2 (deletion of resides 1-22 or 1-40) as shown in Figure 4A. Deletion of either Arg2 amino acids 1-22 or 1-40 resulted in almost exclusive cytoplasmic distribution of Arg2 (Figure 4B and C). A point mutation of the MPP cleavage site at position 36 in Arg2 that was predicted by N-terminal sequencing significantly inhibited the translocation of Arg2 to mitochondria and attenuated Arginase activity.

OxLDL-induced translocation and activation of Arg2 in HAEC involves the Mitochondrial Processing Peptidase (MPP)

The MTS and putative MPP cleavage site in the N-terminus of human Arg 2 that we identified by mass spectrometry and Edman degradation analysis are regions of Arg2 that are highly conserved among species (Figure 5A). Given the redistribution of mitochondrial Arg2 following OxLDL stimulation, we examined whether MPP, and therefore MTS cleavage, contributes to OxLDL-evoked reverse translocation of Arg2 from mitochondria to the cytosol. O-phenanthroline (Oph), a biochemical inhibitor of MPP, prevented the induction of Arg activity (Figure 5B) and completely blocked OxLDL-induced cytosolic release of Arg2 (Figure 5C). Interestingly, the competitive Arg inhibitor 2(S)-amino-6-boronhexanoic acid (ABH), while inhibiting Arginase activity, did not prevent Ox-LDL-induced Arg2 translocation to the cytosol (Figure 5B and 5C). Additionally, MPPα knock down blocked cytosolic redistribution of Arg2 with OxLDL exposure, and prevented Arg2 activation in response to OxLDL (Figure 5D and 5E). On the other hand, control siRNA had no effect on MPP expression, or on the distribution or activity of Arg2. The siRNA for MPP knocked down MPPα subunit protein abundance by more than 50% in HAEC (Figure 5F).

Immunofluorescence localization experiments were then conducted in native vascular endothelial cells in aortic strips from transgenic mice with Tie2 promoter-driven endothelial-specific Arg2 overexpression [33] (Figure 6A). Arg2 was confined to distinct perinuclear granular structures consistent with mitochondria in control samples. Stimulation of the aortic intima with OxLDL resulted in Arg2 redistribution to a diffuse blush consistent with cytoplasmic redistribution, and this was prevented in samples in which MPP was inhibited by OPH. The same redistribution pattern was observed in Arg2-GFP-transduced HAEC (Figure 6B and Supplemental Figure VIII). Additionally, while Arg2 was confined to the mitochondria in quiescent HAEC, OxLDL stimulation led to cytoplasmic translocation, a process that was inhibited by shRNA knockdown of either MPPα or MPPβ in HAEC (Figure 6B).

Inhibition or knockdown of MPP prevents OxLDL-mediated vascular dysfunction and eNOS uncoupling

OxLDL-incubated aortic rings transduced with 100 MOI of control shRNA (NT, nontargeted) exhibited attenuated relaxation responses to acetylcholine (endothelial dysfunction). This was substantially improved in aortic rings that were transduced with either 100 MOI of adenoviruses with shRNA for MPPα or for MPPβ when added 24 hours prior to OxLDL stimulation (Figure 6C and 6D). MPPα and MPPβ knockdown in these vessels was verified by immunoblotting with MPPα and MPPβ specific antibodies (Supplemental Figure V).

The process termed “eNOS uncoupling” occurs under a number of pathologic conditions in which the enzymatic reduction of molecular oxygen by eNOS is no longer coupled to L-arginine oxidation, but leads to an increase in superoxide rather than NO production. OxLDL has been shown to decrease the bioavailability of NO by eNOS uncoupling [34]. This may occur in endothelial cells due to depletion of L-arginine substrate available for eNOS in presence of activated Arg2 [35, 36]. We tested the effects of inhibiting MPP, and its

role in the downstream cytosolic translocation and activation of Arg2, on eNOS uncoupling by OxLDL exposure. MPP inhibition blocked the increased ROS (reactive oxygen species) generation and the decreased NO production seen in aortas from WT (LOX-$1^{+/+}$) mice after OxLDL exposure (Figure 7A and 7B). OxLDL-induction of ROS production in aortas that were not treated with MPP inhibitors was inhibited by L-NAME (100 μM), suggesting that eNOS was the source of ROS (via eNOS uncoupling) in these vessels. OxLDL had no effect on NO production and ROS generation in aortas from LOX-$1^{-/-}$ mice. In addition, endothelium-denuded (E−) strips demonstrated very little ROS production suggesting that the endothelium is the primary source of the OxLDL-dependent ROS (Figure 7C). ROS was measured using the luminol analog L-012, and Nitrite accumulation was measured using a Siever's NO analyzer to determine NO production. The specificity of L-012 for superoxide was examined by treating cells with the superoxide scavenger, SOD (20U/mL). SOD nearly abolished signals from HAEC loaded with L-O12 indicating that chemiluminescence was specific to superoxide (Figure 7D). OxLDL significantly increased superoxide production in HAEC, which was further shown to be sensitive to SOD. Adenoviral knockdown of either Arg 2 or MPPα with human specific shRNA significantly reduced OxLDL-dependent increases in ROS (Fig 7E), and MPPα knockdown obviated the drop in NO that was caused by OxLDL (Fig 7F).

In order to determine whether reduced levels of L-arginine contribute to OxLDL-mediated eNOS uncoupling, we measured the concentration of L-arginine in both the cytosolic and mitochondrial compartments of HAEC in the presence and absence of OxLDL using a Biochrom-20 amino acid analyzer. OxLDL significantly diminished cytosolic L-arginine concentrations (Supplemental Fig IV). Inhibition of MPP with Oph prior to OxLDL exposure prevented this OxLDL-dependent decrease in cytosolic L-arginine.

OxLDL increase MPP activity and is dependent on ROCK

We next used recent data identifying PINK1 cleavage as a metric for MPP activity [37] to interrogate the effects of ROCK and of OxLDL on MPP activity. FLAG-PINK1 cDNA alone or FLAG-PINK1 together with constitutively active (CA) or dominant negative (DN) mutants of ROCK were expressed in HAEC (Supplemental Figure VI). Cleaved PINK1 increased in the presence of CA-ROCK, whereas PINK cleavage did not change when control GFP cDNA or DN-ROCK were co-expressed. The negligible effect observed with DN-ROCK may be attributed to its lower expression level compared to active mutant (third segment of Supplemental Figure VI, panel A). HAEC expressing FLAG-PINK1 were also treated with OxLDL alone or in combination with the ROCK inhibitor Y27632 (Supplemental Figure VI, panel B). OxLDL up regulated PINK1 cleavage (and thus MPP activation), and this was inhibited by Y27632. Taken together, these findings suggest a signaling cascade that is initiated by OxLDL and extends through RhoA and ROCK to MPP.

Arg2 knock out reduces atheromatous plaque burden, improves endothelial function, enhances NO and reduces ROS in ApoE$^{-/-}$ mice

Endothelial dysfunction and inflammation are two critical events that drive atherosclerosis. To investigate the role of Arg2 in endothelial inflammation, we examined OxLDL-dependent NFκB activity in the presence or absence of ABH. NFκB activity was determined

by measuring luciferase activity that was driven by an NFκB response element. OxLDL increased NFκB activity and this was significantly attenuated by ABH (Figure 8A).

Aortic atheromatous plaque burden was then determined in ApoE$^{-/-}$ and Arg2$^{-/-}$/ApoE$^{-/-}$ double knockout mice (DKO) mice (created by backcrossing the Arg2$^{-/-}$ on an ApoE$^{-/-}$ background) that were fed an atherogenic diet for 12 weeks. Plaque thickness was significantly reduced in DKO mice compared to ApoE$^{-/-}$ mice (178.6±25.6 vs. 416.7±52.5 μm, $p < 0.01$; Figure 8B, top and bottom panels) as was the percentage of total aortic surface area that was covered by plaque (38.4±3.8% vs. 52.0±2.8%, n=6, $p < 0.01$; Figure 8C, top and bottom panels). No plaque was detected in WT or Arg2$^{-/-}$ mice.

We next determined vascular reactivity in reponse to acetylcholine (endothelial-dependent) or sodium nitroprusside (endothelial-independent) in isolated aortas from ApoE$^{-/-}$ and DKO mice that were fed a high cholesterol diet/ high fat diet. Endothelial-dependent vascular relaxation in response to acetylcholine was significantly improved in aortas from DKO mice as compared with aortas from ApoE$^{-/-}$ mice (log EC50 = −5.68 ± 0.31, vs. −5.13 ± 0.53 mol/L, $p < 0.05$, n=6). Acetylcholine-mediated relaxation responses in vessels from WT and Arg2$^{-/-}$ mice were significantly greater than in either the ApoE$^{-/-}$ or the DKO samples (log EC50, −5.79±0.23 and −6.05±0.29 mol/L, respectively, $p < 0.05$, n=6) (Figure 8D). eNOS inhibition with L-NAME (100 μM) abolished the relaxation in response to acetylcholine in all groups, suggesting that the differences seen between groups were due to eNOS activity (Supplemental Figure VII). SNP-mediated relaxation (endothelium-independent responses) in samples from WT and Arg2$^{-/-}$ mice were not significantly different than those seen in ApoE$^{-/-}$ or DKO mice (Figure 8E).

We next tested whether genetic deletion of Arg2 ameliorated changes in NO and ROS production that were seen in atheroprone ApoE$^{-/-}$ mice that were fed a high cholesterol diet. Aortic intima from DKO animals exhibited improved NO production and lower ROS levels compared with those measured in samples from ApoE$^{-/-}$ mice (Supplemental Figure IX). The atherogenic diet did not change NO production in Arg2$^{-/-}$ mice (P=0.36).

DISCUSSION

In the current study we show that OxLDL triggers rapid reverse translocation of Arg2 from mitochondria to cytoplasm in EC. This retrograde translocation of Arg2 to cytosol significantly augments its activity, and is dependent upon processing by MPP. Furthermore, using LOX-1$^{-/-}$ KO mice and Rho kinase inhibitors we demonstrate that OxLDL-mediated activation and movement of Arg2 to the cytoplasm is mediated through the LOX-1 receptors on HAEC and requires Rho kinase-mediated signaling. Finally, we show that eNOS uncoupling is a biologically critical consequence of these changes in Arg2 localization and activity, with subsequently reduced NO production and increased generation of ROS.

Many mitochondrial proteins are encoded by nuclear genes, synthesized in the cytosol as large precursor proteins with N-terminal MTSs, and imported into mitochondria [38]. During or after import, precursor proteins may be cleaved by MPP leaving a functional protein [39]. The positively charged MTS are recognized directly by mitochondrial surface receptors and

also facilitate translocation into mitochondria by interacting with the membrane electrical potential that exists across the mitochondrial inner membrane. Some proteins, such as fumarase may undergo bidirectional trafficking between cytosol and mitochondria based upon processing by MPP [40].

Our data indicate that Arg2 is dual-targeted to mitochondria and the cytosol, thereby adding Arg2 to a number of other proteins that share this distinction – up to one quarter of the mitochondrial proteome in some species [41]. There are at least four potential mechanisms by which a single translation product may be present in dual compartments. These include an ambiguous targeting sequence recognized by more than one organelle, multiple targeting sequences; differential targeting accessibility; and reverse translocation - a mechanism that may be dependent upon processing of a MTS in the mitochondria [42]. Our data implicate the latter mechanism in the subcellular trafficking of Arg2. Reverse translocation-based dual targeting of proteins to mitochondria and cytosol in response to altered cellular environment or stress (such as OxLDL exposure) has not been previously described in mammalian cells, and represents a novel mechanism of cellular regulation in health and disease. Data supporting this mechanism in the current study include the demonstrated dependence of localization on both an intact MTS and on the activity of MPP, as the inhibition of MPP in HAEC by either pharmacological or siRNA approaches abolished the cytosolic release and activation of Arg2 in response to OxLDL.

We used experimental data from mass spectrometry and N-terminal sequencing using Edman's degradation analysis followed by genetic mutations to identify and characterize candidates for the MTS and the MPP cleavage site. Differences in the N-terminal residues of cleaved Arg2 that were found by MS and Edman's degradation (HSVAV vs. VHSVAV, respectively) may be explained by post-MPP cleavage “trimming” by other mitochondrial peptidases [43]. Our findings that mutations of the predicted MPP cleavage site inhibited mitochondrial localization of Arg2 and attenuated its activity suggest that processing of Arg2 in mitochondria is a requirement for its activation. This proposed mechanism of dual localization has been characterized in yeast, where the Kreb's cycle enzyme fumarase, is distributed between the mitochondria and cytoplasm based upon metabolic cues from the glycoxylate shunt. The enzyme is first targeted to the mitochondria by an MTS (24 amino acids at the N-terminal sequence) that is processed by MPP. A population of the enzyme then moves back onto the cytoplasm in a process that is regulated by protein folding. One possible mechanism for reverse translocation of Arg2 in the current study is regulation of Arg2 folding by a chaperone protein such as HSP60 - a mitochondrial protein that is released into the cytoplasm in response to endothelial activation with exposure to OxLDL [44] and which we have shown to be a binding partner for Arg2 (unpublished observation).

Despite our finding that the majority of Arg2 is confined to the mitochondria, arginase activity in the cytosol and mitochondrial fractions were comparable. This finding suggests that cytosolic Arg2 is more active than mitochondrial Arg2. This could clarify some controversies regarding the “arginine paradox” -the increased production of NO with addition of extracellular arginine despite saturated levels of intracellular L-arginine [45]. Our findings that the single translation product of Arg2 could be localized in two separate compartments upon cellular stress, and that Arg2 can constrain eNOS activity supports the

concept that specific subcellular pools of L-arginine do exist. We speculate that Arg2 is in closer proximity to binding and/or regulatory proteins that enhance its function after its translocation to cytosol. Recent studies demonstrate that arginine succinate lyase (ASL) enhanced NO production by NOS through recycling citrulline to L-arginine and maintaining the integrity of the NOS complex. Similary, cytosolic ASL could recycle L-citrulline to L-arginine and provide substrate for Arg2 and maintain its structural complex in an active conformation [46].

Activation of Rho kinase has been linked to the acceleration of atherosclerosis in a mouse model [47]. Furthermore, we have demonstrated that RhoA and ROCK are critical to Ox-LDL-dependent increases in EC Arg activity [26]. In the current study, we present data demonstrating that inhibition of ROCK with Y-27632 prevented rises in both cytosolic Arg2 content and activity following Ox-LDL stimulation. These new data suggest that ROCK facilitates Ox-LDL-evoked activation and redistribution of Arg2.

Although it is assumed that the mechanism of eNOS uncoupling by arginase upregulation is in part related to arginase-dependent decrements in L-arginine availability, changes in L-arginine concentrations in response to Ox-LDL have not been measured in individual cellular compartments. Our data demonstrate that Ox-LDL significantly diminished cytosolic L-arginine concentrations (Supplemental Figure IV). These findings are consistent with our hypothesis that Arg2, which is normally confined to the mitochondria, changes to a cytosolic distribution with OxLDL stimulation, and uncouples eNOS in the cytosol. Further, inhibition of MPP both attenuated the increase in cytoplasmic arginase activity and prevented an OxLDL-dependent decrease in cytosolic L-arginine (Figure 5 and Supplemental Figure IV).

In conclusion, the reverse translocation of Arg2 from its MTS-directed sequestration in mitochondria to the cytosol in response to OxLDL apparently underlies a novel mechanism for OxLDL-mediated increases in Arg activity in HAEC. This study identifies MPP as a new subject for targeted therapeutics for atherosclerosis and other vascular disorders in which Arg2 interrupts NO production and promotes the generation of injurious ROS by uncoupling eNOS.

Supplementary Material

Refer to Web version on PubMed Central for supplementary material.

ACKNOWLEDGMENTS

The authors are grateful to Shawna Lewis, Lakshmi Santhanam, Zongming Fu and Nagababu Enika for technical assistance, and to David Fulton of the Vascular Biology Center at Georgia Regents University in Augusta, Georgia for Arg2 cDNA constructs.

SOURCES OF FUNDING

This work was supported by AHA Postdoctoral Fellowship to D.P. (13POST16810011) and HL089668 from NHLBI to D.B. and L.R., by NSF MCB-0923661 to L.R., and by a Clinical Translational Science Award at Johns Hopkins University (JVE) and NIH S10RR024550. This research was supported by Intramural National Institutes of Health Funds from the National Heart Lung and Blood Institute.

Nonstandard Abbreviations and Acronyms

ABH	amino-2-borono-6-hexanoic acid
Arg2	arginase 2
eNOS	endothelial nitric oxide synthase
HAEC	human aortic endothelial cells
MPP	mitochondrial processing peptidase
OxLDL	oxidized low-density lipoprotein
ROCK	rho kinase
ROS	reactive oxygen species
SNP	sodium nitroprusside

REFERENCES

1. Steinberg D. Low density lipoprotein oxidation and its pathobiological significance. J Biol Chem. 1997; 272: 20963–20966. [PubMed: 9261091]
2. Yla-Herttuala S, Palinski W, Rosenfeld ME, Parthasarathy S, Carew TE, Butler S, Witztum JL, Steinberg D. Evidence for the presence of oxidatively modified low density lipoprotein in atherosclerotic lesions of rabbit and man. J Clin Invest. 1989; 84: 1086–1095. [PubMed: 2794046]
3. Ross R. Atherosclerosis--an inflammatory disease. N Engl J Med. 1999; 340: 115–126. [PubMed: 9887164]
4. Galle J, Bengen J, Schollmeyer P, Wanner C. Impairment of endothelium-dependent dilation in rabbit renal arteries by oxidized lipoprotein(a). Role of oxygen-derived radicals. Circulation. 1995; 92: 1582–1589. [PubMed: 7664444]
5. Kugiyama K, Kerns SA, Morrisett JD, Roberts R, Henry PD. Impairment of endothelium-dependent arterial relaxation by lysolecithin in modified low-density lipoproteins. Nature. 1990; 344: 160–162. [PubMed: 2106627]
6. Li H, Forstermann U. Prevention of atherosclerosis by interference with the vascular nitric oxide system. Curr Pharm Des. 2009; 15: 3133–3145. [PubMed: 19754387]
7. Berkowitz DE, White R, Li D, Minhas KM, Cernetich A, Kim S, Burke S, Shoukas AA, Nyhan D, Champion HC, Hare JM. Arginase reciprocally regulates nitric oxide synthase activity and contributes to endothelial dysfunction in aging blood vessels. Circulation. 2003; 108: 2000–2006. [PubMed: 14517171]
8. Closs EI, Simon A, Vekony N, Rotmann A. Plasma membrane transporters for arginine. J Nutr. 2004; 134: 2752S–2759S. [PubMed: 15465780]
9. Haraguchi Y, Takiguchi M, Amaya Y, Kawamoto S, Matsuda I, Mori M. Molecular cloning and nucleotide sequence of cdna for human liver arginase. Proc Natl Acad Sci U S A. 1987; 84: 412–415. [PubMed: 3540966]
10. Morris SM Jr. Bhamidipati D, Kepka-Lenhart D. Human type ii arginase: Sequence analysis and tissue-specific expression. Gene. 1997; 193: 157–161. [PubMed: 9256072]
11. Chang CI, Liao JC, Kuo L. Arginase modulates nitric oxide production in activated macrophages. Am J Physiol. 1998; 274: H342–348. [PubMed: 9458885]
12. Ignarro LJ, Buga GM, Wei LH, Bauer PM, Wu G, del Soldato P. Role of the arginine-nitric oxide pathway in the regulation of vascular smooth muscle cell proliferation. Proc Natl Acad Sci U S A. 2001; 98: 4202–4208. [PubMed: 11259671]

13. Li H, Meininger CJ, Hawker JR Jr. Haynes TE, Kepka-Lenhart D, Mistry SK, Morris SM Jr. Wu G. Regulatory role of arginase i and ii in nitric oxide, polyamine, and proline syntheses in endothelial cells. Am J Physiol Endocrinol Metab. 2001; 280: E75–82. [PubMed: 11120661]

14. Modolell M, Corraliza IM, Link F, Soler G, Eichmann K. Reciprocal regulation of the nitric oxide synthase/arginase balance in mouse bone marrow-derived macrophages by th1 and th2 cytokines. Eur J Immunol. 1995; 25: 1101–1104. [PubMed: 7537672]

15. Morris SM Jr. Kepka-Lenhart D, Chen LC. Differential regulation of arginases and inducible nitric oxide synthase in murine macrophage cells. Am J Physiol. 1998; 275: E740–747. [PubMed: 9814991]

16. Louis CA, Reichner JS, Henry WL Jr. Mastrofrancesco B, Gotoh T, Mori M, Albina JE. Distinct arginase isoforms expressed in primary and transformed macrophages: Regulation by oxygen tension. Am J Physiol. 1998; 274: R775–782. [PubMed: 9530245]

17. Collado B, Sanchez-Chapado M, Prieto JC, Carmena MJ. Hypoxia regulation of expression and angiogenic effects of vasoactive intestinal peptide (vip) and vip receptors in lncap prostate cancer cells. Mol Cell Endocrinol. 2006; 249: 116–122. [PubMed: 16563610]

18. Hein TW, Zhang C, Wang W, Chang CI, Thengchaisri N, Kuo L. Ischemia-reperfusion selectively impairs nitric oxide-mediated dilation in coronary arterioles: Counteracting role of arginase. Faseb J. 2003; 17: 2328–2330. [PubMed: 14563685]

19. Jung C, Gonon AT, Sjoquist PO, Lundberg JO, Pernow J. Arginase inhibition mediates cardioprotection during ischaemia-reperfusion. Cardiovasc Res. 2010; 85: 147–154. [PubMed: 19726439]

20. Zhang C, Hein TW, Wang W, Miller MW, Fossum TW, McDonald MM, Humphrey JD, Kuo L. Upregulation of vascular arginase in hypertension decreases nitric oxide-mediated dilation of coronary arterioles. Hypertension. 2004; 44: 935–943. [PubMed: 15492130]

21. Johnson FK, Johnson RA, Peyton KJ, Durante W. Arginase inhibition restores arteriolar endothelial function in dahl rats with salt-induced hypertension. Am J Physiol Regul Integr Comp Physiol. 2005; 288: R1057–1062. [PubMed: 15591155]

22. Peyton KJ, Ensenat D, Azam MA, Keswani AN, Kannan S, Liu XM, Wang H, Tulis DA, Durante W. Arginase promotes neointima formation in rat injured carotid arteries. Arterioscler Thromb Vasc Biol. 2009; 29: 488–494. [PubMed: 19164802]

23. Ryoo S, Gupta G, Benjo A, Lim HK, Camara A, Sikka G, Lim HK, Sohi J, Santhanam L, Soucy K, Tuday E, Baraban E, Ilies M, Gerstenblith G, Nyhan D, Shoukas A, Christianson DW, Alp NJ, Champion HC, Huso D, Berkowitz DE. Endothelial arginase ii: A novel target for the treatment of atherosclerosis. Circ Res. 2008; 102: 923–932. [PubMed: 18309100]

24. Ryoo S, Lemmon CA, Soucy KG, Gupta G, White AR, Nyhan D, Shoukas A, Romer LH, Berkowitz DE. Oxidized low-density lipoprotein-dependent endothelial arginase ii activation contributes to impaired nitric oxide signaling. Circ Res. 2006; 99: 951–960. [PubMed: 17008605]

25. Ming XF, Barandier C, Viswambharan H, Kwak BR, Mach F, Mazzolai L, Hayoz D, Ruffieux J, Rusconi S, Montani JP, Yang Z. Thrombin stimulates human endothelial arginase enzymatic activity via rhoa/rock pathway: Implications for atherosclerotic endothelial dysfunction. Circulation. 2004; 110: 3708–3714. [PubMed: 15569838]

26. Ryoo S, Bhunia A, Chang F, Shoukas A, Berkowitz DE, Romer LH. Oxldl-dependent activation of arginase ii is dependent on the lox-1 receptor and downstream rhoa signaling. Atherosclerosis. 2011; 214: 279–287. [PubMed: 21130456]

27. Levillain O, Balvay S, Peyrol S. Mitochondrial expression of arginase ii in male and female rat inner medullary collecting ducts. J Histochem Cytochem. 2005; 53: 533–541. [PubMed: 15805427]

28. Lim HK, Lim HK, Ryoo S, Benjo A, Shuleri K, Miriel V, Baraban E, Camara A, Soucy K, Nyhan D, Shoukas A, Berkowitz DE. Mitochondrial arginase ii constrains endothelial nos-3 activity. Am J Physiol Heart Circ Physiol. 2007; 293: H3317–3324. [PubMed: 17827260]

29. Lucas R, Czikora I, Sridhar S, Zemskov EA, Oseghale A, Circo S, Cederbaum SD, Chakraborty T, Fulton DJ, Caldwell RW, Romero MJ. Arginase 1: An unexpected mediator of pulmonary capillary barrier dysfunction in models of acute lung injury. Frontiers in immunology. 2013; 4: 228. [PubMed: 23966993]

30. Kubli DA, Gustafsson AB. Mitochondria and mitophagy: The yin and yang of cell death control. Circ Res. 2012; 111: 1208–1221. [PubMed: 23065344]

31. Li M, Zhong Z, Zhu J, Xiang D, Dai N, Cao X, Qing Y, Yang Z, Xie J, Li Z, Baugh L, Wang G, Wang D. Identification and characterization of mitochondrial targeting sequence of human apurinic/apyrimidinic endonuclease 1. J Biol Chem. 2010; 285: 14871–14881. [PubMed: 20231292]

32. Niidome T, Kitada S, Shimokata K, Ogishima T, Ito A. Arginine residues in the extension peptide are required for cleavage of a precursor by mitochondrial processing peptidase. Demonstration using synthetic peptide as a substrate. J Biol Chem. 1994; 269: 24719–24722. [PubMed: 7929146]

33. Vaisman BL, Andrews KL, Khong SM, Wood KC, Moore XL, Fu Y, Kepka-Lenhart DM, Morris SM Jr. Remaley AT, Chin-Dusting JP. Selective endothelial overexpression of arginase ii induces endothelial dysfunction and hypertension and enhances atherosclerosis in mice. PLoS One. 2012; 7: e39487. [PubMed: 22829869]

34. Fleming I, Mohamed A, Galle J, Turchanowa L, Brandes RP, Fisslthaler B, Busse R. Oxidized low-density lipoprotein increases superoxide production by endothelial nitric oxide synthase by inhibiting pkcalpha. Cardiovasc Res. 2005; 65: 897–906. [PubMed: 15721870]

35. Khong SM, Andrews KL, Huynh NN, Venardos K, Aprico A, Michell DL, Zarei M, Moe KT, Dusting GJ, Kaye DM, Chin-Dusting JP. Arginase ii inhibition prevents nitrate tolerance. Br J Pharmacol. 2012; 166: 2015–2023. [PubMed: 22288373]

36. Kim JH, Bugaj LJ, Oh YJ, Bivalacqua TJ, Ryoo S, Soucy KG, Santhanam L, Webb A, Camara A, Sikka G, Nyhan D, Shoukas AA, Ilies M, Christianson DW, Champion HC, Berkowitz DE. Arginase inhibition restores nos coupling and reverses endothelial dysfunction and vascular stiffness in old rats. J Appl Physiol (1985). 2009; 107: 1249–1257. [PubMed: 19661445]

37. Greene AW, Grenier K, Aguileta MA, Muise S, Farazifard R, Haque ME, McBride HM, Park DS, Fon EA. Mitochondrial processing peptidase regulates pink1 processing, import and parkin recruitment. EMBO reports. 2012; 13: 378–385. [PubMed: 22354088]

38. Schmidt O, Pfanner N, Meisinger C. Mitochondrial protein import: From proteomics to functional mechanisms. Nat Rev Mol Cell Biol. 2010; 11: 655–667. [PubMed: 20729931]

39. Neupert W, Herrmann JM. Translocation of proteins into mitochondria. Annu Rev Biochem. 2007; 76: 723–749. [PubMed: 17263664]

40. Stein I, Peleg Y, Even-Ram S, Pines O. The single translation product of the fum1 gene (fumarase) is processed in mitochondria before being distributed between the cytosol and mitochondria in saccharomyces cerevisiae. Mol Cell Biol. 1994; 14: 4770–4778. [PubMed: 8007976]

41. Dinur-Mills M, Tal M, Pines O. Dual targeted mitochondrial proteins are characterized by lower mts parameters and total net charge. PLoS One. 2008; 3: e2161. [PubMed: 18478128]

42. Regev-Rudzki N, Yogev O, Pines O. The mitochondrial targeting sequence tilts the balance between mitochondrial and cytosolic dual localization. J Cell Sci. 2008; 121: 2423–2431. [PubMed: 18577574]

43. Teixeira PF, Glaser E. Processing peptidases in mitochondria and chloroplasts. Biochim Biophys Acta. 2013; 1833: 360–370. [PubMed: 22495024]

44. Grundtman C, Kreutmayer SB, Almanzar G, Wick MC, Wick G. Heat shock protein 60 and immune inflammatory responses in atherosclerosis. Arterioscler Thromb Vasc Biol. 2011; 31: 960–968. [PubMed: 21508342]

45. Kurz S, Harrison DG. Insulin and the arginine paradox. J Clin Invest. 1997; 99: 369–370. [PubMed: 9022065]

46. Erez A, Nagamani SC, Shchelochkov OA, Premkumar MH, Campeau PM, Chen Y, Garg HK, Li L, Mian A, Bertin TK, Black JO, Zeng H, Tang Y, Reddy AK, Summar M, O'Brien WE, Harrison DG, Mitch WE, Marini JC, Aschner JL, Bryan NS, Lee B. Requirement of argininosuccinate lyase for systemic nitric oxide production. Nat Med. 2011; 17: 1619–1626. [PubMed: 22081021]

47. Shimokawa H, Morishige K, Miyata K, Kandabashi T, Eto Y, Ikegaki I, Asano T, Kaibuchi K, Takeshita A. Long-term inhibition of rho-kinase induces a regression of arteriosclerotic coronary lesions in a porcine model in vivo. Cardiovasc Res. 2001; 51: 169–177. [PubMed: 11399259]

Novelty and Significance

What Is Known?

- Arginase 2 (Arg2) inhibits nitric oxide (NO) production by endothelial nitric oxide synthase (eNOS) by competing for the common substrate L-arginine.
- In quiescent endothelial cells Arg2 is confined predominantly to the mitochondria.
- Activation of endothelial cells by the atherogenic stimulus oxidized lLDL) leads to a rapid increase in arginase activity, and this results in eNOS uncoupling and contributes to endothelial dysfunction.
- Pharmacologic inhibition of arginase improves NO production and endothelial function, and reduces plaque burden in atheroprone ApoE$^{-/-}$ mice.

What New Information Does This Article Contribute?

- oxLDl induces reverse translocation of Arg2 reverse from mitochondria to the cytoplasm where Arg2 constrains eNOS activity.
- OxLDL-mediated translocation of Arg2 is dependent upon the presence of a mitochondrial targeting sequenc in Arg2, and the mitochondrial processing peptidase.
- Knockout of Arg 2 in atherogenic ApoE$^{-/-}$ mice recouples eNOS to its substrate L-arginine, improves endothelial function, and reduces atherosclerotic plaque burden.

Arginase is an important negative regulator of eNOS because of its competition for the common substrate L-arginine. Arginase upregulation contributes to the pathobiology of vascular diseases including atherosclerosis, erectile dysfunction, and pulmonary and systemic hypertension. OxLDL-mediated injury to endothelium causes 2 distinct events that contribute to increased Arg2: a decreased check on Arg2 transcription by HDAC 2; and a rapid increase in Arg2 activity. In this paper we report that OxLDL triggers rapid Arg2 translocation from the mitochondria of EC (where it is confined in the quiescent state) to their cytosol. This process requires the LOX-1 receptor, Rho kinase, and MPP. Arg2 translocation leads to eNOS uncoupling, decreased NO production, and impaired endothelial-dependent vasorelaxation. Finally Arg2$^{-/-}$ mice bred on an ApoE$^{-/-}$ background exhibit enhanced eNOS function, improved endothelium-mediated vasoreactivity, and reduced plaque load. These findings suggest a novel mechanism for rapid Arg2 activation in response to EC injury; and reveal a signaling pathway by which a single gene product with an unambiguous mitochondrial targeting sequence undergoes dual compartmentalization.

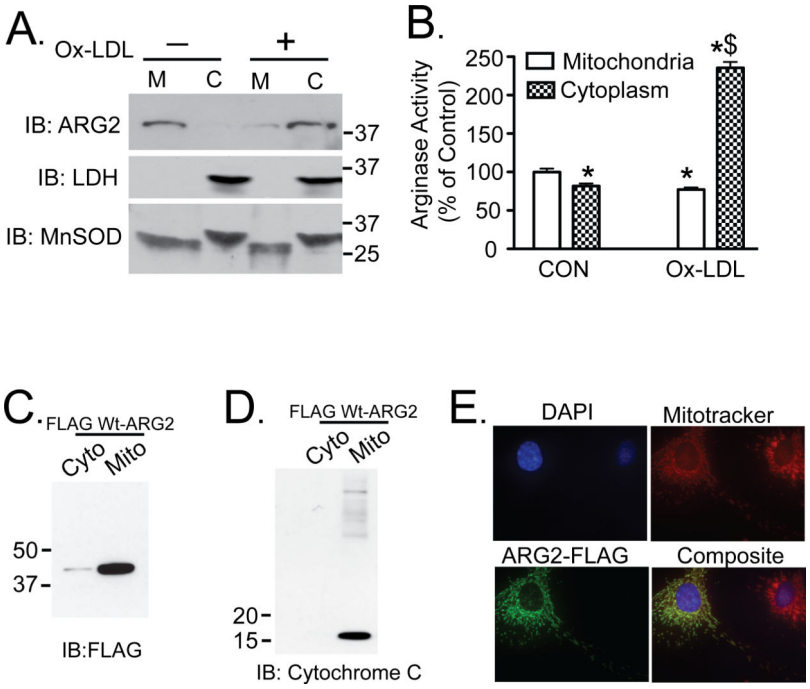

Figure 1. Ox-LDL triggers cytosolic release of activated Arg 2

HAEC were incubated with 50μg/ml Ox-LDL for 2h. Cell lysates were fractionated by differential centrifugation. **A.** The quantity of Arg2 was measured in cytosolic (C) and mitochondrial fractions (M) by western blotting. Cell lysates were also immunoblotted for LDH and MnSOD to verify fractionation. **B.** Arginase activity was measured in the separated C and M fractions. **C. and D.** 293 cells were transfected with C-terminal FLAG epitope-tagged Arg2 and subjected to cytosolic and mitochondrial fractionation. Fractionated lysates were probed with FLAG antibody (**C**), and with cytochrome C antibody (**D**). **E.** FLAG-Arg2-transfected unstimulated HAEC were stained with mitotracker red CMXRos (red), anti-Flag primary antibody, AlexaFlour 488 mouse (green) secondary, and DAPI (blue) and analyzed by immunoflorescence. * denotes $p<0.05$ vs Control group (CON, panel B).

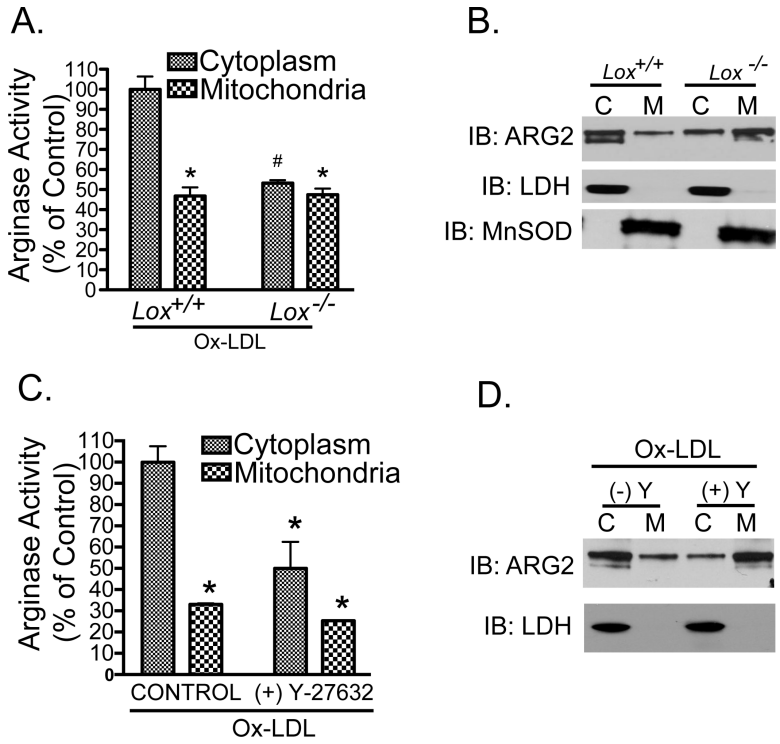

Figure 2. Ox-LDL-mediated activation and cytosolic release of Arg2 require LOX-1 and Rho kinase signaling

A and B: Endothelial cells were isolated from WT and LOX-1 knockout (LOX-1$^{-/-}$) murine aortas and incubated with 50μg/ml Ox-LDL for 2h. Mitochondrial and cytosolic fractions were separated for measurements of Arginase activity **(A)** and immunoblotting for Arg2 **(B)**. **C and D:** In other experiments, HAEC were exposed to either OxLDL alone or OxLDL with Y-27632. Mitochondrial and cytosolic fractions were used for arginase activity measurements **(C)**, or immunoblotting for Arg2 **(D)**. * denotes P<0.05 vs control group.

A.

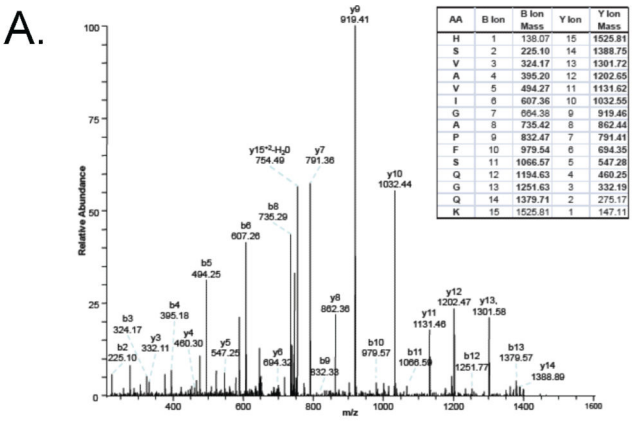

AA	B Ion	B Ion Mass	Y Ion	Y Ion Mass
H	1	138.07	15	1525.81
S	2	225.10	14	1388.75
V	3	324.17	13	1301.72
A	4	395.20	12	1202.65
V	5	494.27	11	1131.62
I	6	607.36	10	1032.55
G	7	664.38	9	919.46
A	8	735.42	8	862.44
P	9	832.47	7	791.41
F	10	979.54	6	694.35
S	11	1066.57	5	547.28
Q	12	1194.63	4	460.25
G	13	1251.63	3	332.19
Q	14	1379.71	2	275.17
K	15	1525.81	1	147.11

B.

Panel A) N-terminal amino acid sequence by N-terminal Edman Degradation
(Intact full length Arginase 2 is blocked at the N-terminus and so will not be sequenced, only degraded or cleaved forms with free N-termini will be sequenced by this technique)

Sequence round								
1	2	3	4	5	6	7	8	9
V	H	S	V	A	V	I	G	A
S	Q	-	-	-	A	-	-	-
A	-	-	-	-	-	-	-	-

Panel B) Human Arginase 2, with potential mitochondrial targeting sequence(s)

MSLRGSLSRL LQTRVHSILK KSVHSVAVIG APFSQGQKRK GVEHGPAAIR EAGLMKRLSS
LGCHLKDFGD LSFTPVPKDD LYNNLIVNPR SVGLANQELA EVVSRAVSDG YSCVTLGGDH
SLAIGTISGH ARHCPDLCVV WVDAHADINT PLTTSSGNLH GQPVSFLLRE LQDKVPQLPG
FSWIKPCISS ASIVYIGLRD VDPPEHFILK NYDIQYFSMR DIDRLGIQKV MERTFDLLIG
KRQRPIHLSF DIDAFDPTLA PATGTPVVGG LTYREGMYIA EEIHNTGLLS ALDLVEVNPQ
LATSEEEAKT TANLAVDVIA SSFGQTREGG HIVYDQLPTP SSPDESENQA RVRI

Figure 3. Cytosolic Arg2 is truncated

A.) Collision-induced dissociation (CID) fragmentation spectra of a 762.73 [M+2H] ion from a tryptic in-gel digest of Arg2 that was immunoprecipitated from the cytoplasm of OxLDL-treated HAEC using an anti-Arg2 polyclonal antibody. **B)** Cell lysates from Flag-tagged Arg2-transfected 293 cells were immunoprecipitated with Flag monoclonal antibody and subjected to N-terminal Edman degradation analysis.

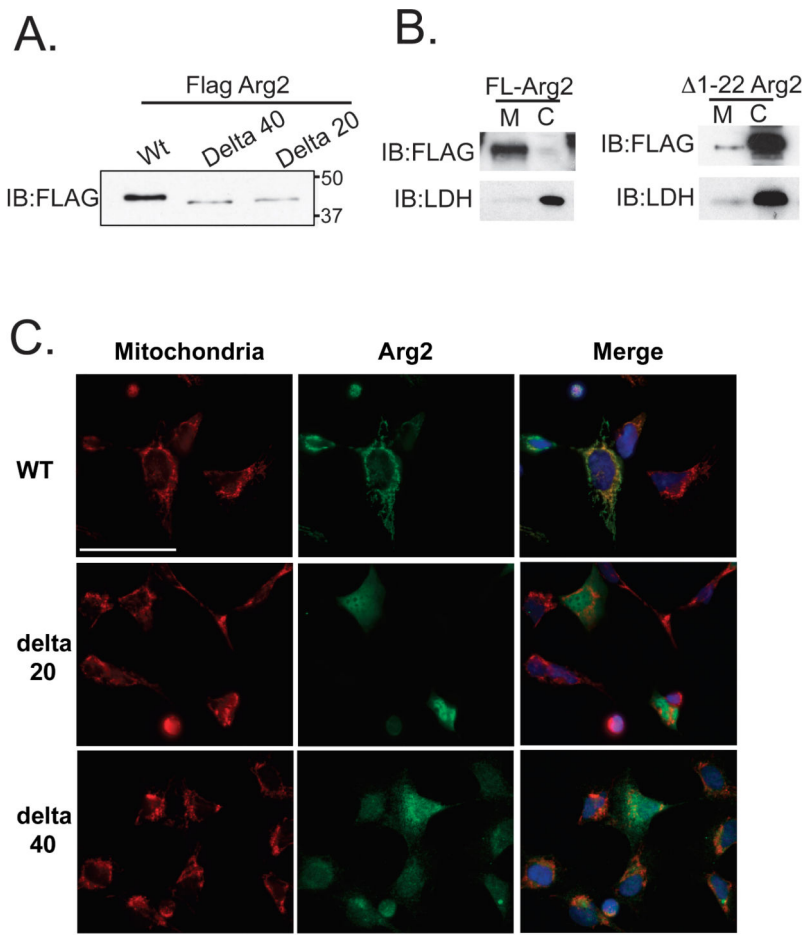

Figure 4. The MTS of Arg2 is located on N-terminus and includes amino acids 1-22 or 1-40

HAEC were transfected with Full length Arg2, or either the 1-22 or the 1-40 N terminal deletion mutants, and analysis of A) western blotting, B) subcellular fractionation of full length and 1-22 truncated Arg2, and C) immunofluorescence using anti-FLAG antibody (green) and mitotracker red are shown. Full length Arg2 was localized almost exclusively to mitochondria and both truncated mutants were predominantly cytosolic (DAPI-labeled nuclei (blue) are shown in the merged images). Scale bar denotes ~40 microns.

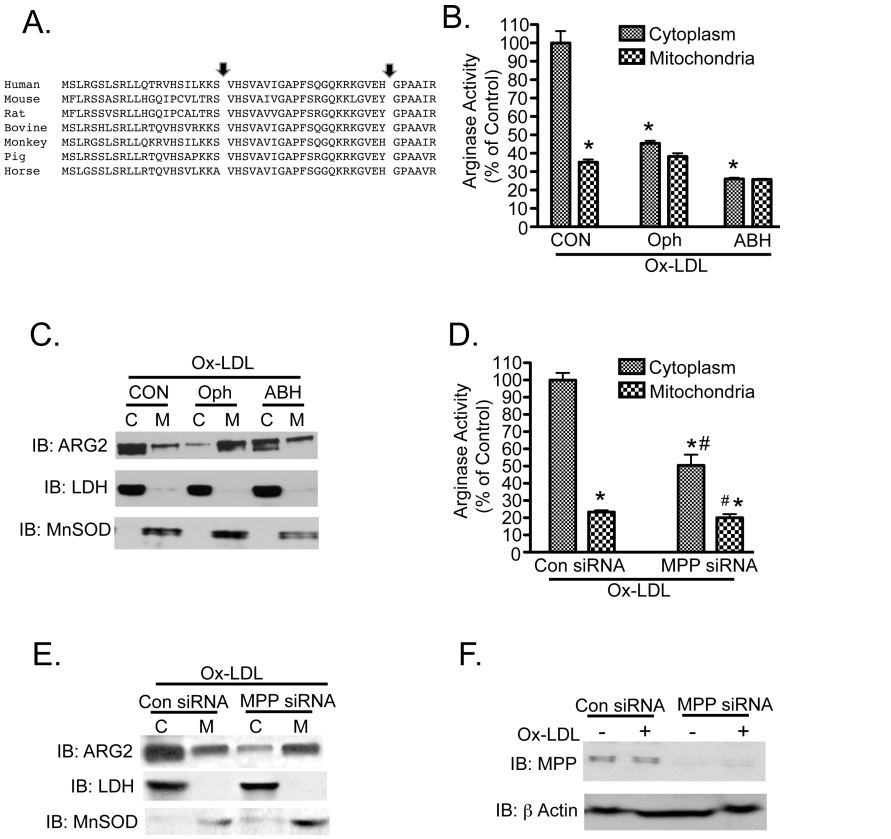

Figure 5. Pharmacologic inhibition or siRNA-mediated knockdown of MPP prevent activation and release of Arg2 to cytosol

A) N-terminal Arg2 protein sequences from several species were aligned utilizing the Clustal W method and Mac Vector software. **B and C**: Serum-starved HAEC were pre-incubated with 5mM O-phenanthroline or 100nM ABH for 30 min to inhibit MPP or arginase activity, respectively. Cells were then incubated with 50μg/ml Ox-LDL for 2h and then fractionated. Arginase activity **(B)**, and Arg2 protein expression **(C)** were measured in the mitochondrial (M) and cytosolic (C) fractions. **D-F**: MPP-specific siRNA (10nM) was transfected into HAEC. Serum-starved cells were then treated with OxLDL for 2h, and subjected to fractionation. Arginase activity **(D)** and Arg2 expression **(E)** were measured in C and M fractions. Knockdown efficiency of the MPP siRNA was determined by immunoblotting for MPP in both untreated and OxLDL-treated HAEC (F). * indicates $p<0.05$ vs. Control cytosolic group, and # denotes $p<0.05$ vs. Control mitochondrial group.

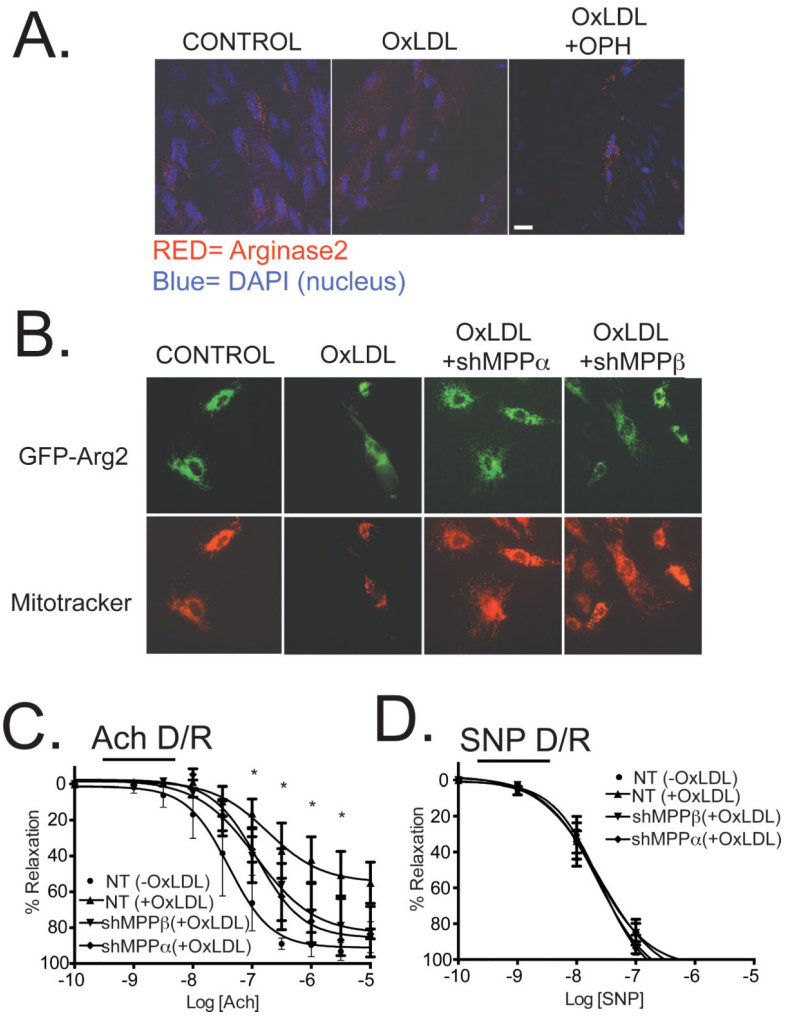

Figure 6. OxLDL-mediated redistribution of Arg2 and impairment of endothelial function are prevented by biochemical inhibition of MPP and by MPPα or MPPβ knockdown

A) Confocal images from aortic strips isolated from Arg2-overexpressing mice are shown: Left panel shows untreated controls; Middle panel shows effects of 50μg/mL of OxLDL; Right panel shows effects of 1mM of Oph for 30m prior to the 2h treatment with 50μg/mL OxLDL. Data are representative of three independent experiments. B) After transduction with non-targeted, MPPα shRNA or MPPβ shRNA, HAEC were further transduced with GFP-tagged Arg2 (C-term). 24 hours later cells were incubated in presence or absence of 50μg/ml Ox-LDL for 2 hours and subjected to immunofluorescence for GFP-Arg2 and Mitotracker. C and D) Murine aortic rings were incubated with 100 MOI of nontargeted, MPPα or MPPβ shRNA adenoviruses and treated 24 hours later with or without OxLDL (50μg/mL). Dose-response effects of ACh (C) and SNP (D) on vascular relaxation were then determined. * indicates $p<0.05$ vs. Control (NT/-OxLDL).

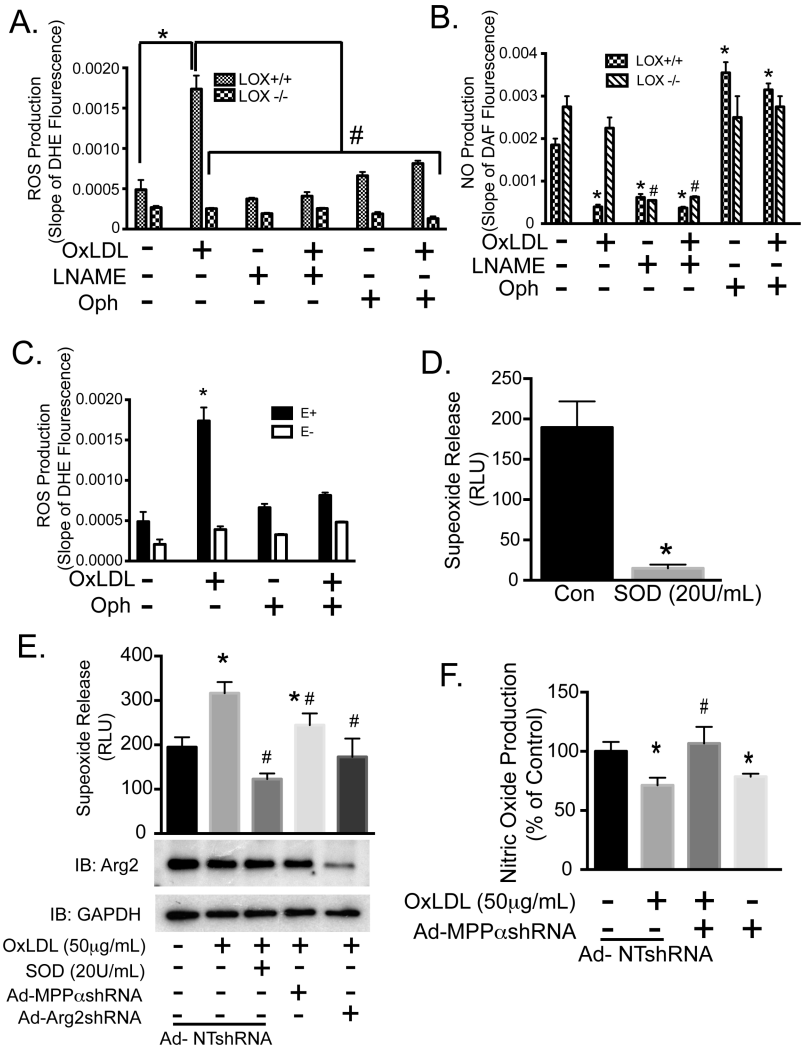

Figure 7. Ox-LDL-mediated eNOS uncoupling is dependent upon MPP and intact endothelium

Aortic strips from wild type or LOX-1$^{-/-}$ mice were exposed to OxLDL alone, OxLDL with 5mM Oph, or OxLDL plus L-NAME (100μM). A) ROS production was measured as the slope of DHE fluorescence. B) NO production was measured as a slope of DAF fluorescence. C) ROS production was also studied in parallel in murine aortic specimens with intact (E+) or mechanically denuded (E−) intimal endothelium. D) HAEC production of ROS was determined by L-012 chemiluminescence following incubation with or without SOD (20U/mL), and expressed as relative light units (RLU). E) HAEC were incubated with 100 MOI of nontargeted, MPPα or MPPβ shRNA adenoviruses. 24 hours after transduction, media was replaced with fresh media with or without OxLDL (50μg/mL). After 48 hours, the production of ROS was determined in presence or absence of SOD (20U/mL) via L-012 chemiluminescence. F) HAEC were incubated with 100 MOI of nontargeted shRNA or MPPα shRNA adenoviruses. Cells were treated the next day with control medium or OxLDL (50μg/mL). After 48 hours, the production of NO was determined by measuring nitrite levels with Siever's NO analyzer, means ± S.E are shown, n=6. * indicates $p<0.05$ vs. Con, # denotes $p<0.05$ vs. OxLDL.

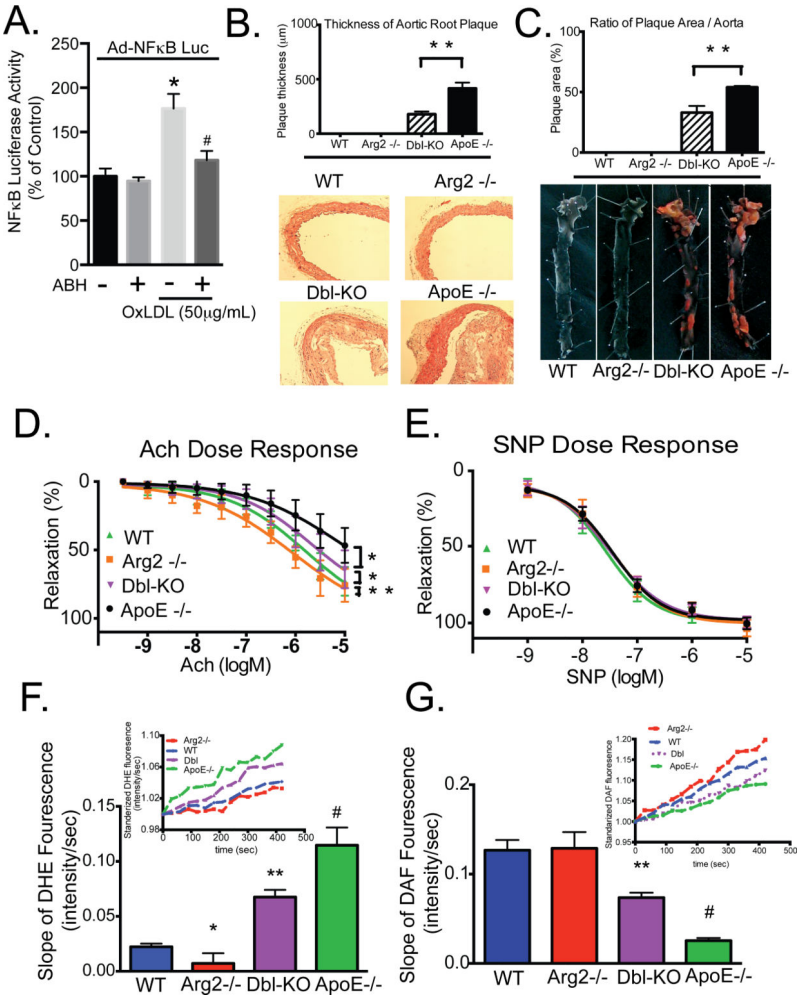

Figure 8. Arg2 inhibition ameliorates atherogenesis in ApoE knockout mice

A) HAEC expressing NFkB-LUC were incubated with OxLDL (50μg/mL) alone or with ABH (200μM) for 8 hours, and luciferase activity was determined using chemiluminescence. B) Quantitative graph (upper panel) of plaque formation in histological sections of ascending aortas (lower panel). C) Cumulative quantitative assessment (upper panel) of the plaque area determined by pixel count of Sudan IV-stained areas of the lipid-rich intraluminal lesions in longitudinally opened aortas (lower panel). D and E) Dose-response effects of Ach (D) and SNP (E) on vascular relaxation in isolated aortas from $ApoE^{-/-}$ mice and Dbl-KO ($ArgII^{-/-}/ApoE^{-/-}$) mice fed with HC diet were determined. * indicates P<0.05 vs Con, ** indicates P<0.001, # indicates P<0.05 vs OxLDL without ABH.